Mathematical Biosciences and Engineering

http://www.aimspress.com/journal/mbe

MBE, 21(1): 1249–1269.
DOI: 10.3934/mbe.2024053
Received: 13 October 2023
Revised: 01 December 2023
Accepted: 06 December 2023
Published: 26 December 2023

Research article

A practical approach to computing Lyapunov exponents of renewal and delay equations

Dimitri Breda and Davide Liessi*

CDLab – Computational Dynamics Laboratory, Department of Mathematics, Computer Science and Physics, University of Udine, Via delle Scienze 206, 33100 Udine, Italy

* **Correspondence:** Email: davide.liessi@uniud.it.

Abstract: We propose a method for computing the Lyapunov exponents of renewal equations (delay equations of Volterra type) and of coupled systems of renewal and delay differential equations. The method consists of the reformulation of the delay equation as an abstract differential equation, the reduction of the latter to a system of ordinary differential equations via pseudospectral collocation and the application of the standard discrete QR method. The effectiveness of the method is shown experimentally and a MATLAB implementation is provided.

Keywords: Lyapunov exponents; delay equations; renewal equations; pseudospectral collocation; discrete QR method; abstract differential equation

1. Introduction

A delay equation is a functional equation consisting of "a rule for extending a function of time towards the future on the basis of the (assumed to be) known past" [1]. A renewal equation (RE) is a delay equation of Volterra type, i.e., the rule for extension prescribes the value of the unknown function itself, instead of the value of its derivative, as in the case of delay differential equations (DDEs).

The goal of this work is to compute the (dominant) Lyapunov exponents (LEs) of REs and of coupled systems of REs and DDEs (henceforth *coupled* equations). The usefulness of LEs for measuring the asymptotic exponential behavior of solutions is well known; for example, they can be used to study the average asymptotic stability of solutions, the insurgence of chaotic dynamics and the effects of perturbations on the system, as well as to estimate the entropy or the dimension of attractors.

As for DDEs, recent methods for computing the LEs have been proposed, particularly [2] and [3], which use two different approaches (for other methods, see the references in the cited works).

In [3] the DDE is reformulated as an abstract differential equation and a pseudospectral discretization is applied [4], yielding a system of ordinary differential equations (ODEs); LEs are then computed

by using the standard discrete QR method (henceforth *DQR*) for ODEs proposed in [5, 6]. In [2], instead, the problem is tackled directly: the DDE is posed in an infinite-dimensional Hilbert space as the state space, the associated family of evolution operators is discretized and the DQR is adapted and applied to the finite-dimensional approximation; for the error analysis, the DQR is raised to infinite dimension and compared to the approximated DQR used for the computations.

As for REs, as far as we know, there are no methods available in the literature for computing LEs. Only a first example of naive computation can be found in [7], where it is done simply to exemplify the versatility of the collocation techniques used therein, without attempting a rigorous formulation and error analysis.

In the present work of computational nature, we develop a practical method following the approach of [3] described above, and based on [8] for the reformulation of REs into abstract differential equations. As in [3], we use the DQR to compute the LEs of the approximating ODE, but, in principle, any method can be used; our choice was motivated by our goal of providing a practical way of computing LEs by using ready-to-use code for a well-known method.

In Section 2 we recall the DQR for linear ODEs. Then, in Section 3 we define the reformulation of REs, DDEs and coupled equations into abstract differential equations and their pseudospectral collocation into ODEs. After describing the implementation choices in Section 4, we present in Section 5 some numerical experiments concerning the convergence of the method for an example RE with many known properties, as well as some examples of computation of LEs of REs and coupled equations. Finally, we present some concluding remarks in Section 6.

The MATLAB codes implementing the method and the scripts to reproduce the experiments of Section 5 are available at `http://cdlab.uniud.it/software`.

2. DQR for ODEs

In this section, we first illustrate the DQR to compute the LEs of linear nonautonomous ODEs; in the nonlinear case, one previously linearizes around a reference trajectory in the attractor. Then, we comment on the relevant literature.

Let n be a positive integer and consider the ODE

$$z'(t) = A(t)z(t) \tag{2.1}$$

for $A\colon [0, +\infty) \to \mathbb{R}^{n\times n}$ continuous and bounded; also, let $Z(t)$ be the fundamental matrix solution exiting from a given nonsingular matrix $Z_0 \in \mathbb{R}^{n\times n}$ prescribed at time 0 without loss of generality. For any sequence $\{t_k\}_{k\in\mathbb{N}}$ of time instants strictly increasing from $t_0 = 0$, construct the iterative QR factorization[1]

$$Z(t_k) = Q_k R_k \tag{2.2}$$

starting from $Z_0 = Q_0R_0$ and, at each step $j = 1, \dots, k$, solving the n initial value problems (IVPs)

$$\begin{cases} \Gamma'(t, t_{j-1}) = A(t)\Gamma(t, t_{j-1}), \quad t \in [t_{j-1}, t_j], \\ \Gamma(t_{j-1}, t_{j-1}) = Q_{j-1} \end{cases} \tag{2.3}$$

[1]In what follows, a QR factorization of a nonsingular matrix is intended as the unique one with positive diagonal elements.

and factorizing the solution at t_j as

$$\Gamma(t_j, t_{j-1}) = Q_j R_{j,j-1}. \tag{2.4}$$

If $S(t, s) \coloneqq Z(t)Z(s)^{-1}$ is the state transition matrix associated with (2.1), then

$$\begin{aligned} Z(t_k) &= S(t_k, t_{k-1}) \cdots S(t_2, t_1) S(t_1, t_0) Q_0 R_0 \\ &= S(t_k, t_{k-1}) \cdots S(t_2, t_1) \Gamma(t_1, t_0) R_0 \\ &= S(t_k, t_{k-1}) \cdots S(t_2, t_1) Q_1 R_{1,0} R_0 \\ &= S(t_k, t_{k-1}) \cdots \Gamma(t_2, t_1) R_{1,0} R_0 \\ &= S(t_k, t_{k-1}) \cdots Q_2 R_{2,1} R_{1,0} R_0 \\ &\cdots \\ &= Q_k R_{k,k-1} \cdots R_{1,0} R_0. \end{aligned}$$

The uniqueness of the QR factorization and (2.2) give

$$R_k = \left(\prod_{j=1}^{k} R_{j,j-1} \right) R_0,$$

so that, eventually, (upper[2]) LEs are recovered as

$$\lambda_i = \limsup_{k \to \infty} \frac{1}{t_k} \sum_{j=1}^{k} \ln [R_{j,j-1}]_{i,i}, \quad i = 1, \ldots, n. \tag{2.5}$$

Above, $[R_{j,j-1}]_{i,i}$ denotes the i-th diagonal entry of the j-th triangular factor $R_{j,j-1}$. Obviously, in the implementation (2.5) is truncated to some large $T > 0$. In the end, each step of the DQR requires the solution of the IVPs (2.3) and the QR factorization (2.4).

The above summary was taken mainly from [3], where the DQR is applied to the ODE obtained from the pseudospectral collocation of a given DDE (see Section 3), thus following the original approach of [4] to also address the study of chaotic dynamics. As anticipated in Section 1, the aim of the present work is to extend this procedure to more general classes of delay equations, such as REs and coupled equations. Once the pseudospectral collocation is performed (possibly after linearization, see Remark 4.1 later on), the outcome is an ODE like (2.1); thus, the DQR applies unchanged, independent of the original delay equation.

The literature on the theory and computation of LEs of ODEs is ample; for a starting reference, see [12], but see also [9] as a reference monograph. QR methods were first proposed in the pioneering works [13, 14]; for a complete discussion of the discrete version, see [6]. The literature on the computation of LEs of delay equations is mostly of an experimental flavor and, to the best of the authors' knowledge, restricted only to DDEs. As initial references, we can suggest [2, 15, 16], but see also

[2]Lower exponents come either as lim inf or as upper exponents of the adjoint system. Note, however, that for *regular* ODEs in the sense of Lyapunov (see, e.g., [9, Definition 3.5.1]) the LEs exist as exact limits, and such quantities are meaningful for stability statements in the original nonlinear system, thus avoiding the so-called Perron effect (see, e.g., [10]). Nevertheless, an in-depth study of the theoretical requirements of the original delay equation guaranteeing the regularity of the ODE obtained by pseudospectral collocation is beyond the scope of the present work, as well as the extension of the regularity concept itself to the infinite-dimensional case of delay equations (extension that the authors, to the best of their knowledge, are not aware of; see, anyway, [11] and the references therein).

[17] for a more recent method to reduce DDEs to ODEs by using Galerkin-type projections. Note also that all of these works rely on a Hilbert state space setting to legitimize orthogonal projections, while the technique in [3] is free from this constraint and thus maintains the classical state spaces (typically continuous functions for DDEs and absolutely integrable ones for REs). Beyond the lack of relevant methods, this is part of the motivation for the extension of the approach proposed in [3] to more general delay equations.

3. Pseudospectral collocation

In this section, we illustrate the use of pseudospectral collocation to reduce delay equations to ODEs, in view of the application of the DQR described in Section 2. For the reader's convenience, we first present, separately, the discretization of an RE in Section 3.1 and that of a DDE in Section 3.2, summarizing from, respectively, [8] and [3] the main aspects for the present objective (for a full treatment, see again [3, 8] and also [4]). Eventually, we combine the two approaches in Section 3.3 for a coupled equation.

In what follows, we use the subscripts X and Y to refer, respectively, to REs and DDEs.

3.1. Pseudospectral collocation of REs

Let $\tau > 0$ be real and $d_X > 0$ be an integer. Consider the IVP for an RE given by

$$\begin{cases} x(t) = F(x_t), & t > 0, \\ x(\theta) = \phi(\theta), & \theta \in [-\tau, 0], \end{cases} \tag{3.1}$$

where $\phi \in L^1 := L^1([-\tau, 0]; \mathbb{R}^{d_X})$, $F\colon L^1 \to \mathbb{R}^{d_X}$ and x_t, defined as $x_t(\theta) := x(t + \theta)$ for $\theta \in [-\tau, 0]$, denotes the history or state function (so that $x_0 = \phi$ represents the initial state). If F is globally Lipschitz, the IVP (3.1) has a unique solution on $[-\tau, +\infty)$ [18, Theorem 3.8].

In [8] an efficient application of pseudospectral collocation to reduce (3.1) to an IVP for an ODE is proposed based on an equivalent formulation of (3.1) as an abstract Cauchy problem (ACP) describing the evolution of an integral of the original state x_t. In particular, by defining the Volterra integral operator $\mathcal{V}\colon L^1 \to AC_0$ as

$$(\mathcal{V}\eta)(\theta) := -\int_\theta^0 \eta(s)\,\mathrm{d}s,$$

where $AC_0 := AC_0([-\tau, 0]; \mathbb{R}^{d_X})$ is the space[3] of absolutely continuous functions vanishing at 0, it turns out that (3.1) is equivalent to the ACP

$$\begin{cases} u'(t) = \mathcal{A}_{0,X}u(t) + q_X F(\mathcal{A}_{0,X}u(t)), & t \geq 0, \\ u(0) = \mathcal{V}\phi \end{cases} \tag{3.2}$$

through $u(t) = \mathcal{V}x_t$. Above, $\mathcal{A}_{0,X}\colon \mathcal{D}(\mathcal{A}_{0,X}) \subset NBV_0 \to NBV_0$ is defined as $(\mathcal{V}_{\restriction_{NBV_0}})^{-1}$, i.e.,

$$\mathcal{A}_{0,X}\mu := \mu', \qquad \mathcal{D}(\mathcal{A}_{0,X}) := \{\mu \in AC_0 : \mu = \mathcal{V}\eta \text{ for some } \eta \in NBV_0\}, \tag{3.3}$$

[3]Hereinafter, we do not indicate the domain and codomain of a function space when clear from the context.

where NBV_0 is the space of functions of bounded variation vanishing at 0 and continuous from the right, and $q_X \in NBV_0$ is defined as

$$q_X(\theta) \coloneqq \begin{cases} 0, & \theta = 0, \\ -1, & \theta \in [-\tau, 0). \end{cases}$$

In order to discretize (3.2), consider a mesh $\Omega_{M_X,X}$ of M_X points $-\tau \le \theta_{M_X,X} < \cdots < \theta_{1,X} < 0$ with M_X a positive integer. Correspondingly, let $P_{M_X,X}\colon \mathbb{R}^{M_X d_X} \to NBV_0$ be the interpolation operator on $\{0\} \cup \Omega_{M_X,X}$ with value 0 at $\theta_{0,X} \coloneqq 0$, i.e.,

$$(P_{M_X,X}\Phi)(\theta) \coloneqq \sum_{j=1}^{M_X} \ell_{j,X}(\theta)\Phi_j, \quad \theta \in [-\tau, 0],$$

where $\{\ell_{0,X}, \ell_{1,X}, \dots, \ell_{M_X,X}\}$ is the Lagrange basis on $\{0\} \cup \Omega_{M_X,X}$, and let $R_{M_X,X}\colon NBV_0 \to \mathbb{R}^{M_X d_X}$ be the restriction operator

$$(R_{M_X,X}\mu)_j \coloneqq \mu(\theta_{j,X}), \quad j = 1, \dots, M_X.$$

Then, the discrete version of (3.2) is given by

$$\begin{cases} U'(t) = D_{M_X,X}U(t) - \mathbf{1}_{M_X,X}F_{M_X}(U(t)), & t \ge 0, \\ U(0) = R_{M_X,X}\mathcal{V}\phi, \end{cases} \tag{3.4}$$

with $U(t) \in \mathbb{R}^{M_X d_X}$ that approximates the integrated state $\mathcal{V}x_t$ according to $U_j(t) \approx (\mathcal{V}x_t)(\theta_{j,X})$, $j = 1, \dots, M_X$,[4] and where $D_{M_X,X} \coloneqq R_{M_X,X}\mathcal{A}_{0,X}P_{M_X,X} \in \mathbb{R}^{M_X d_X \times M_X d_X}$ has $d_X \times d_X$-block entries

$$[D_{M_X,X}]_{i,j} = \ell'_{j,X}(\theta_{i,X})I_{d_X}, \quad i, j = 1, \dots, M_X,$$

where I_{d_X} is the identity on $\mathbb{R}^{d_X}$, $F_{M_X} \coloneqq F \circ \mathcal{A}_{0,X}P_{M_X,X}$ and $\mathbf{1}_{M_X,X} \in \mathbb{R}^{M_X d_X \times d_X}$ has all $d_X \times d_X$-block entries I_{d_X}.[5]

Remark 3.1. *Instead of NBV_0, [8] uses the space NBV of functions of bounded variation that vanish at* 0 *and are continuous from the right on $(-\tau, 0)$, but not necessarily at $-\tau$. In that setting, $C_{0,X} \coloneqq (\mathcal{V}_{\restriction_{NBV}})^{-1}$ is a multi-valued operator, defined as*[6] *$C_{0,X}\mu \coloneqq \{\eta : \mu = V\eta\}$, since functions differing only by the jump at $-\tau$ are mapped by $\mathcal{V}$ to the same element of NBV. The* trivial *semigroup $\{S_{0,X}(t)\}_{t\ge 0}$ on NBV defined as*

$$S_{0,X}(t)\colon NBV \to NBV, \qquad (S_{0,X}(t)\mu)(\theta) \coloneqq \begin{cases} \mu(t+\theta), & t+\theta \le 0, \\ 0, & t+\theta > 0, \end{cases}$$

is not strongly continuous. However, its restriction $\{T_{0,X}(t)\}_{t\ge 0}$ to AC_0 is strongly continuous and $\mathcal{A}_{0,X}$ is its infinitesimal generator.

From this point of view, the semilinear ACP (3.2) *renders a clear separation between the* translation along the solutions *(through the linear semigroup $\{T_{0,X}(t)\}_{t\ge 0}$ and its infinitesimal generator $\mathcal{A}_{0,X}$) and the* rule for extension *(basically through the nonlinear right-hand side F of the specific RE), which are the two ingredients of a delay equation. For these and related aspects of the theory of delay equations, see [18, 19] for the sun–star ($\odot*$) theory and [1, 8] for the more recent twin semigroup theory.*

[4] Note then that $\mathcal{A}_{0,X}P_{M_X,X}U(t) \approx x_t$.
[5] Note that $\mathbf{1}_{M_X,X}$ discretizes $-q_X$.
[6] It turns out that $D(C_{0,X}) = D(\mathcal{A}_{0,X})$ (see (3.3)).

3.2. Pseudospectral collocation of DDEs

Let $\tau > 0$ be real and $d_Y > 0$ be an integer. Consider the IVP for a DDE given by

$$\begin{cases} y'(t) = G(y_t), & t \geq 0, \\ y(\theta) = \psi(\theta), & \theta \in [-\tau, 0], \end{cases} \tag{3.5}$$

where $\psi \in C := C([-\tau, 0]; \mathbb{R}^{d_Y})$, $G\colon C \to \mathbb{R}^{d_Y}$ and y_t is defined as x_t in Section 3.1 (so, again, $y_0 = \psi$ represents the initial state). If G is globally Lipschitz, the IVP (3.5) has a unique solution on $[-\tau, +\infty)$ [20, Section 2.2].

In [3] (but see also [4]) pseudospectral collocation is used to reduce (3.5) to an IVP for an ODE based on an equivalent formulation of (3.5) as an ACP describing the evolution of the original state y_t, viz.

$$\begin{cases} v'(t) = \mathcal{A}_Y v(t), & t \geq 0, \\ v(0) = \psi \end{cases} \tag{3.6}$$

through $v(t) = y_t$. Above, $\mathcal{A}_Y\colon \mathcal{D}(\mathcal{A}_Y) \subset C \to C$ is defined as

$$\mathcal{A}_Y \rho := \rho', \qquad \mathcal{D}(\mathcal{A}_Y) := \{\rho \in C : \rho' \in C \text{ and } \rho'(0) = G(\rho)\}.$$

In order to discretize (3.6), consider a mesh $\Omega_{M_Y,Y}$ of $1 + M_Y$ points $-\tau = \theta_{M_Y,Y} < \theta_{M_Y-1,Y} < \cdots < \theta_{1,Y} < \theta_{0,Y} := 0$ with M_Y a positive integer. Correspondingly, let $P_{M_Y,Y}\colon \mathbb{R}^{(1+M_Y)d_Y} \to C$ be the interpolation operator on $\Omega_{M_Y,Y}$, i.e.,

$$(P_{M_Y,Y}\Psi)(\theta) := \sum_{j=0}^{M_Y} \ell_{j,Y}(\theta)\Psi_j, \quad \theta \in [-\tau, 0],$$

where $\{\ell_{0,Y}, \ell_{1,Y}, \ldots, \ell_{M_Y,Y}\}$ is the Lagrange basis on $\Omega_{M_Y,Y}$, and let $R_{M_Y,Y} : C \to \mathbb{R}^{(1+M_Y)d_Y}$ be the restriction operator

$$(R_{M_Y,Y}\rho)_j := \rho(\theta_{j,Y}), \quad j = 0, 1, \ldots, M_Y.$$

Then, the discrete version of (3.6) is given by

$$\begin{cases} V_0'(t) = G_{M_Y}(V(t)), & t \geq 0, \\ V_j'(t) = D_{M_Y,Y}V(t), & t \geq 0, \ j = 1, \ldots, M_Y, \\ V(0) = R_{M_Y,Y}\psi, \end{cases} \tag{3.7}$$

for $V(t) \in \mathbb{R}^{(1+M_Y)d_Y}$ that approximates the state y_t according to $V_j(t) \approx (y_t)(\theta_{j,Y})$, $j = 0, 1, \ldots, M_Y$, and where $D_{M_Y,Y}$ has $d_Y \times d_Y$-block entries

$$[D_{M_Y,Y}]_{i,j} = \ell_{j,Y}'(\theta_{i,Y})I_{d_Y}, \quad i = 1, \ldots, M_Y, \ j = 0, 1, \ldots, M_Y,$$

where I_{d_Y} is the identity on $\mathbb{R}^{d_Y}$ and $G_{M_Y} := G \circ P_{M_Y,Y}$.

Remark 3.2. *Note that the ACP* (3.6) *can be alternatively described as the equivalent semilinear ACP*

$$\begin{cases} v'(t) = \mathcal{A}_{0,Y}v(t) + q_Y G(v(t)), & t \geq 0, \\ v(0) = \psi, \end{cases} \tag{3.8}$$

where $\mathcal{A}_{0,Y}$ is the infinitesimal generator of the shift *semigroup $\{T_{0,Y}(t)\}_{t\geq 0}$ defined as*

$$T_{0,Y}(t)\colon C \to C, \qquad (T_{0,Y}(t)\rho)(\theta) \coloneqq \begin{cases} \rho(t+\theta), & t+\theta \leq 0, \\ \rho(0), & t+\theta > 0, \end{cases}$$

and $q_Y \in L^\infty$ is defined as

$$q_y(\theta) \coloneqq \begin{cases} 1, & \theta = 0, \\ 0, & \theta \in [-\tau, 0). \end{cases}$$

Equation (3.8) *renders for DDEs the same separation between* translation along the solutions *and* rule for extension *as illustrated in Remark 3.1 for REs (see again [19]). The pseudospectral collocation of* (3.8) *leads, again, to* (3.7)*, which can be rewritten equivalently as*

$$\begin{cases} V'(t) = D_{0,M_Y,Y}V(t) + \mathbf{1}_{M_Y,Y}G_{M_Y}(U(t), V(t)), & t \geq 0, \\ V(0) = R_{M_Y,Y}\psi, \end{cases} \tag{3.9}$$

where $D_{0,M_Y,Y}$ is as $D_{M_Y,Y}$ but with an additional d_Y-block row of zeros; also, $\mathbf{1}_{M_Y,Y} \in \mathbb{R}^{(1+M_Y)d_Y \times d_Y}$ has the first $d_Y \times d_Y$-block equal to I_{d_Y} and all of the others equal to zero. Now, (3.9) *resembles* (3.8).

3.3. Pseudospectral collocation of coupled equations

Let τ, d_X and d_Y be as above. Consider the IVP for a coupled equation given by

$$\begin{cases} x(t) = F(x_t, y_t), & t > 0, \\ y'(t) = G(x_t, y_t), & t \geq 0, \\ x(\theta) = \phi(\theta), & \theta \in [-\tau, 0], \\ y(\theta) = \psi(\theta), & \theta \in [-\tau, 0], \end{cases} \tag{3.10}$$

where $\phi \in L_1$, $\psi \in C$, $F\colon L^1 \times C \to \mathbb{R}^{d_X}$ and $G\colon L^1 \times C \to \mathbb{R}^{d_Y}$. For well-posedness, see [18].

By combining the approaches of the previous sections, it follows that (3.10) is equivalent to the ACP

$$\begin{cases} (u'(t), v'(t)) = \mathcal{B}_{X,Y}(u(t), v(t)), & t \geq 0, \\ (u(0), v(0)) = (\mathcal{V}\phi, \psi), \end{cases} \tag{3.11}$$

with $\mathcal{B}_{X,Y}\colon \mathcal{D}(\mathcal{B}_{X,Y}) \subset NBV_0 \times Y \to NBV_0 \times Y$ defined as

$$\mathcal{B}_{X,Y}(\phi, \psi) \coloneqq (\mathcal{A}_{0,X}\phi + q_X F(\mathcal{A}_{0,X}\phi, \psi), \psi'),$$
$$\mathcal{D}(\mathcal{B}_{X,Y}) \coloneqq \{(\varphi, \psi) \in \mathcal{D}(\mathcal{A}_{0,X}) \times Y : \psi' \in Y,\ \psi'(0) = G(\mathcal{A}_{0,X}\phi, \psi)\},$$

through $(u(t), v(t)) = (\mathcal{V}x_t, y_t)$.

The discrete version of (3.11) is as follows:

$$\begin{cases} U'(t) = D_{M_X,X}U(t) - \mathbf{1}_{M_X,X}F_{M_X}(U(t), V(t)), & t \geq 0, \\ V_0'(t) = G_{M_Y}(U(t), V(t)), & t \geq 0, \\ V_j'(t) = D_{M_Y,Y}V(t), & t \geq 0,\ j = 1, \ldots, M_Y, \\ U(0) = R_{M_X,X}\mathcal{V}\phi, \\ V(0) = R_{M_Y,Y}\psi. \end{cases} \tag{3.12}$$

Note that, now, $F_{M_X} \coloneqq F \circ (\mathcal{A}_{0,X}P_{M_X,X}, P_{M_Y,Y})$ and $G_{M_Y} \coloneqq G \circ (\mathcal{A}_{0,X}P_{M_X,X}, P_{M_Y,Y})$. The total number of approximating ODEs is $M_X d_X + (1 + M_Y)d_Y$, which becomes $(2M + 1)d$ if $d_X = d_Y = d$ and $M_X = M_Y = M$.

Remark 3.3. *Following Remarks 3.1 and 3.2, it is not difficult to see that* (3.11) *is equivalent to the semilinear ACP*

$$\begin{cases} (u'(t), v'(t)) = \mathcal{A}_{0,X,Y}(u(t), v(t)) + \mathcal{N}_{X,Y}(u(t), v(t)), \quad t \geq 0, \\ (u(0), v(0)) = (\mathcal{V}\phi, \psi), \end{cases} \tag{3.13}$$

where $\mathcal{A}_{0,X,Y} \coloneqq \operatorname{diag}(\mathcal{A}_{0,X}, \mathcal{A}_{0,Y})$ *is linear and*

$$\mathcal{N}_{X,Y}(\phi, \psi) \coloneqq (q_X F(\mathcal{A}_{0,X}\phi, \psi), q_Y G(\mathcal{A}_{0,X}\phi, \psi))$$

is nonlinear. The pseudospectral collocation of (3.13) *leads, again, to* (3.12)*, where, correspondingly, the ODEs for V can be compacted as done in Remark 3.2 for DDEs; see* (3.9)*. The (numerical) analysis of* (3.13) *is current work in progress at CDLab,*[7] *also in view of the corresponding sun–star theory of coupled equations developed in [18] and of the more recent twin semigroup theory of [1].*

4. Implementation

Due to our choice of example equations (see Section 5), in our implementation we considered scalar equations ($d_X = d_Y = 1$) of the following kinds:

$$x(t) = \int_{-\tau_2}^{-\tau_1} f(x(t + \theta))\, \mathrm{d}\theta \tag{4.1}$$

for REs, and

$$\begin{cases} x(t) = y(t) \displaystyle\int_{-\tau_2}^{-\tau_1} f_1(x(t + \theta))\, \mathrm{d}\theta, \\ y'(t) = g(y(t)) + y(t) \displaystyle\int_{-\tau_2}^{-\tau_1} f_2(x(t + \theta))\, \mathrm{d}\theta, \end{cases} \tag{4.2}$$

for coupled equations,[8] where $\tau_2 > \tau_1 > 0$, and f, f_1, f_2 and g are (possibly) nonlinear functions $\mathbb{R} \to \mathbb{R}$. Nevertheless, generalizing to other forms of equations is usually fairly straightforward.[9]

We implemented the pseudospectral discretization[10] using Chebyshev nodes of type II (extrema) as the meshes $\{0\} \cup \Omega_{M_X,X}$ and $\Omega_{M_Y,Y}$ of points in $[-\tau, 0]$ with $M_X = M_Y$. To compute the nodes and the corresponding differentiation matrix, we used the `cheb` routine of [22, Chapter 6]. For the interpolation, we used the barycentric Lagrange interpolation formula [23]; the barycentric weights corresponding to Chebyshev extrema are explicitly known and are given therein. For the quadrature of the integrals, we used the Clenshaw–Curtis formula [24, 25]. We implemented $(\mathcal{A}_{0,X}P_{M_X,X}\Phi)(\theta)$ as

[7] `http://cdlab.uniud.it/`

[8] Observe that the unknown of the differential equation is not delayed.

[9] For instance, one can consider models such as (3.3) in [21], yet with finite age-span, which do not enter class (4.2). In such cases, the method is implemented following the same strategy described here (discretization of the nonlinear system for computing solutions, linearization and discretization of the linearized system for computing the LEs). However, the authors are currently implementing a general code for a larger class of equations (ideally the most general (3.10)), which was beyond the scope of this work.

[10] For more details on pseudospectral methods, see also [22].

$\sum_{j=1}^{M_X} \ell'_{j,X}(\theta)\Phi_j$, computing $\ell'_{j,X}$ as the polynomial interpolating the j-th column of the differentiation matrix, again with the barycentric formula.

In order to apply the DQR described in Section 2 to the approximating ODE, the latter needs to be linearized around a reference solution. The linearization is done explicitly. The solutions are computed by using MATLAB's `ode45`, which implements the embedded Dormand–Prince (5, 4) method [26, 27]. For the differential part of (4.2), the initial value consists of the vector of values of the chosen initial function at $\Omega_{M_Y,Y}$, while, for (4.1) and the renewal part of (4.2), the vector $D^{-1}_{M_X,X}u$ is used,[11] where u is the vector of values of the initial function at $\Omega_{M_X,X}$.

Finally, the DQR for a linear ODE is implemented in the `dqr` routine of [3], which follows [5]. Therein, the IVPs (2.3) are again solved with the Dormand–Prince (5, 4) pair; however, instead of adapting the step size (initially 0.01) based on the error between the two solutions, the automatic adaptation controls the error between the corresponding LEs. As an initial guess for the fundamental matrix solution, a random matrix is used. The computation is stopped when the specified truncation time T is reached.

Remark 4.1. *For REs only, and in particular for the example described in Section 5.1, we experimented also with a different method, based on computing a solution of* (4.1)*, linearizing the latter around the former and applying the pseudospectral collocation to the resulting linear RE. We computed the solution of the RE with the method described in [28], which is based on the trapezoidal quadrature formula on a uniform grid in* $[-\tau_2, 0]$ *with the constraint that* $-\tau_1$ *must be a grid point. Corresponding to a solution* $\bar{x}$*, we considered the linear RE*[12]

$$x(t) = \int_{-\tau_2}^{-\tau_1} f'(\bar{x}(t+\theta))x(t+\theta)\,\mathrm{d}\theta. \tag{4.3}$$

See Section 5.1 for a comparison of the approaches.

Remark 4.2. *In Remark 4.1 (more precisely in Footnote 12), we observed that, in most cases, REs cannot be linearized. However, in many of those cases, the ODE resulting from the pseudospectral discretization can, in fact, be linearized; for example, the ODEs resulting from* (4.1) *and* (4.2) *can be linearized if* f*,* f_1*,* f_2 *and* g *are differentiable. As an example, the linearization of* (3.12) *around a solution* $(\overline{U}, \overline{V})$ *is as follows:*

$$\begin{cases} U'(t) = D_{M_X,X}U(t) - \mathbf{1}_{M_X,X} \cdot JF_{M_X}(\overline{U}(t), \overline{V}(t)) \cdot (U(t), V(t))^T, \\ V'_0(t) = JG_{M_Y}(\overline{U}(t), \overline{V}(t)) \cdot (U(t), V(t))^T, \\ V'_j(t) = D_{M_Y,Y}V(t), \quad j = 1, \dots, M_Y, \end{cases}$$

[11] In (3.4) the initial value is specified as $R_{M_X,X}\mathcal{V}\phi$, i.e., the vector representing the polynomial interpolating the exact integral of the initial value ψ. Another approach is to use $R_{M_X,X}\mathcal{V}P_{M_X,X}R_{M_X,X}\phi$, in which the integral of the polynomial interpolating ψ is used. In our implementation we use neither; our choice is computationally easier and is motivated as follows.

As already noted, in order to represent the integrated state, only the vector U of values at $\Omega_{M_X,X}$ is needed, as the value at $\theta_{0,X} = 0$ is always 0. Computing the derivative of the interpolating polynomial by applying the differentiation matrix to $(0, U)^T$ (where the 0 stands for a column vector of d_X zeros), we obtain $(d_{M_X,X}U, D_{M_X,X}U)^T$, where $d_{M_X,X} \in \mathbb{R}^{d_X \times M_X d_X}$ is a row of $d_X \times d_X$-block entries $\ell'_{j,X}(\theta_{0,X})I_{d_X}$ for $j = 1, \dots, M_X$. Since deriving a polynomial lowers its degree by one, $D_{M_X,X}U$ uniquely determines the derivative of the polynomial represented by U, which motivates our use of $D^{-1}_{M_X,X}u$.

[12] In general, (4.3) may actually not be the linearization of (4.1) around $\bar{x}$ in L^1. Indeed, the right-hand side of the equation is *not* Fréchet-differentiable unless f is affine. See [18, Section 3.5] for details, in particular with respect to studying the stability of equilibria; the extension of the results therein is an open problem.

where J indicates the Jacobian matrix, $JF_{M_X}(\overline{U}(t), \overline{V}(t))$ is a $d_X \times (M_X d_X + (1 + M_Y)d_Y)$ matrix and $JG_{M_Y}(\overline{U}(t), \overline{V}(t))$ is a $d_Y \times (M_X d_X + (1 + M_Y)d_Y)$ matrix. In Section 5.1 below, we explicitly show the linearized ODE for an example RE.

We recall that the MATLAB codes implementing the method and the scripts to reproduce the experiments of Section 5 are available at `http://cdlab.uniud.it/software`.

5. Results

We present here three example equations: an RE with a quadratic (logistic-like) nonlinearity in Section 5.1, an RE modeling egg cannibalism in Section 5.2 and a simplified version of the Daphnia model with a logistic term for the growth of the resource in Section 5.3. In particular, we use the first example to test the proposed method also from the numerical point of view; we then apply it to the second and third example to compute the exponents.

5.1. RE with quadratic nonlinearity

The first equation we study is the RE with quadratic nonlinearity from [7]:

$$x(t) = \frac{\gamma}{2} \int_{-3}^{-1} x(t+\theta)(1 - x(t+\theta))\, \mathrm{d}\theta, \tag{5.1}$$

i.e., (4.1) with $\tau_1 := 1$, $\tau_2 := 3$ and $f(x) := \frac{\gamma}{2} x(1 - x)$. Its equilibria and their stability properties are known; in particular, its nontrivial equilibrium undergoes a Hopf bifurcation for $\gamma = 2 + \frac{\pi}{2}$ and the branch of periodic solutions arising from there has the analytic expression

$$\bar{x}(t) = \frac{1}{2} + \frac{\pi}{4\gamma} + \sqrt{\frac{1}{2} - \frac{1}{\gamma} - \frac{\pi}{2\gamma^2}\Big(1 + \frac{\pi}{4}\Big)}\, \sin\Big(\frac{\pi}{2} t\Big). \tag{5.2}$$

Observe that the period is 4, independent of γ. Moreover, it is experimentally known that it presents several period-doubling bifurcations, possibly leading to a cascade and, eventually, to chaos [7].

Since several properties of (5.1) are analytically known, we use it to test the effectiveness and efficiency of the method proposed for LE computation, and to compare it to the alternative approach described in Remark 4.1.

For equilibria, the LEs are the real parts of the eigenvalues λ of the infinitesimal generator of the semigroup of solution operators, which are related to the eigenvalues μ of the solution operator that advances the solution by h via

$$\mu = \mathrm{e}^{\lambda h}. \tag{5.3}$$

For periodic solutions, the LEs are the real parts of the Floquet exponents, which are related to the Floquet multipliers (i.e., the eigenvalues of the monodromy operator) via (5.3), where μ, λ and h are, respectively, a Floquet multiplier, a Floquet exponent and the period. In both cases, we can thus obtain the LEs by computing the eigenvalues μ of an evolution operator with any time step h for the equilibria (we choose $h = \tau_2 = 3$ for (5.1)) and a time step h equal to the period for periodic solutions ($h = 4$ for (5.2)), and then computing the real part of $\log(\mu)/h$. In order to obtain reference values for our

experiments, we compute the spectra of evolution operators with the method of [29], which is based on the pseudospectral collocation of the operator; we use the implementation `eigTMNpw` of [30, 31].

Although computing the solutions of delay equations is not the focus of this work, given that both the main approach and the alternative one of Remark 4.1 involve computing solutions, our first experiment compares the error of the computed solutions with respect to the known periodic solutions of (5.1). We choose $\gamma = 4 > 2 + \frac{\pi}{2}$, which corresponds to a stable periodic solution, since the first period-doubling bifurcation is experimentally known to happen at $\gamma \approx 4.32$ [7, 29].

Figure 1 shows the errors on the solution of the approximating ODE and on the solution of the original RE (5.1) with respect to the number of nodes (minus 1) in the grid in $[-3, 0]$, i.e., M_X for the pseudospectral discretization and $3r$ for the trapezoidal method[13] [28]; in both cases, two errors are measured, namely the absolute error at $t = 500$ and the maximum absolute error on a grid of points in $[0, 500]$ (a uniform grid with step 0.05 for the pseudospectral approach, the time points given by the trapezoidal method for the alternative approach). To solve the approximating ODE given by the pseudospectral discretization, we used `ode45` with `RelTol` $= 10^{-6}$ and `AbsTol` $= 10^{-7}$, which justifies the barrier on the error in Figure 1.

The experiment confirms that the trapezoidal method has order 2, as proved in [28], and that the pseudospectral discretization has infinite order, which is often the case for pseudospectral methods applied to smooth problems [22]. Even for rather small values of $M_X = 3r$, the error for the pseudospectral method is several orders of magnitudes smaller than the one for the trapezoidal method.[14]

In the next experiment, we investigate how the errors on the LEs depend on the choice of M_X and of the final time[15] T. We choose values of γ corresponding to the stable trivial equilibrium ($\gamma = 0.5$), the stable nontrivial equilibrium ($\gamma = 3$) and the stable periodic orbit ($\gamma = 4$).

Since we are going to use the linearization of the ODE (3.4) coming from the RE (5.1), as an example, we show it explicitly here. With reference to Remark 4.2, observe that the right-hand side of (5.1) is not Fréchet-differentiable as a map from L^1 to $\mathbb{R}$, while the right-hand side of the discretized equation is differentiable. The linearization of the approximating ODE around the solution $\overline{U}$ is given by

$$U'(t) = D_{M_X,X}U(t) - \mathbf{1}_{M_X,X} \cdot JF_{M_X}(\overline{U}(t)) \cdot U(t),$$

where $JF_{M_X}(\overline{U}(t))$ is a row vector with components

$$[JF_{M_X}(\overline{U}(t))]_j = \frac{\gamma}{2} \int_{-3}^{-1} \left(1 - 2 \sum_{k=1}^{M_X} \ell'_{k,X}(\theta)\overline{U}_k(t)\right) \ell'_{j,X}(\theta)\, \mathrm{d}\theta, \quad j = 1, \ldots, M_X.$$

In Figures 2 and 3, we can see the absolute errors on the dominant LE increasing either M_X or T. The tolerance for `dqr` is 10^{-6}, while those for `ode45` are `RelTol` $= 10^{-6}$ and `AbsTol` $= 10^{-7}$. The

[13] As noted in Remark 4.1, $-\tau_1 = -1$ must be a grid point in $[-\tau_2, 0] = [-3, 0]$; we thus choose the number r of nodes (minus 1) in $[-\tau_1, 0]$ as the discretization parameter for the trapezoidal method [28], resulting in $3r + 1$ nodes in total.

[14] As already noted, computing the solutions is not the focus of the present work. Admittedly, there are other more sophisticated methods in the literature: see, e.g., [32, 33, 34]. However, in most cases, they are not readily applicable to (4.1) and (4.2), due to the discontinuity in the integration kernel at $-\tau_1$, when the integral is considered on the interval $[-\tau_2, 0]$; in other cases, the implementation of the method is not available and is not as straightforward as [28]. It is worth mentioning that pseudospectral methods for computing periodic solutions of REs and coupled equations, exhibiting the usual infinite order of convergence, are available in [35, 36, 37]; they are based on solving the corresponding boundary value problem, so they cannot be straightforwardly adapted to computing generic solutions.

[15] Observe that the `dqr` routine does not stop exactly at T, but at the first time step exceeding T, i.e., it does not refine the final step.

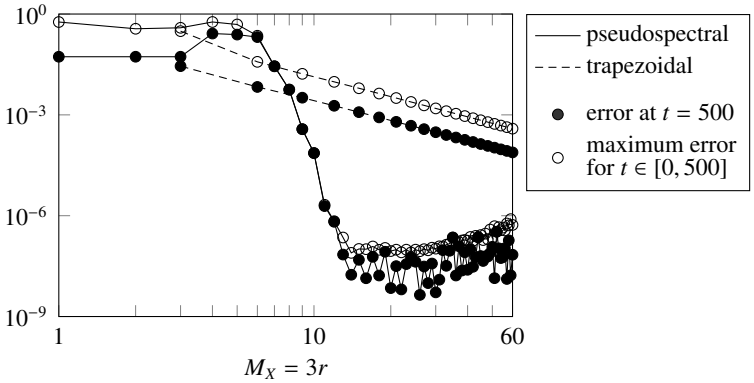

Figure 1. Errors on the solution of the RE with quadratic nonlinearity (5.1) with $\gamma = 4$ with respect to the known periodic solution (5.2), computed via pseudospectral discretization (solid lines) and directly with the trapezoidal method (dashed lines), measured as the absolute error at $t = 500$ (•) and as the maximum absolute error on a grid of points in $[0, 500]$ (∘), when varying the number of nodes (minus 1) in the grid in $[-3, 0]$, i.e., M_X for the pseudospectral discretization and $3r$ for the trapezoidal method. The exact periodic solution (5.2) is used as the initial value.

reference values are obtained by using `eigTMNpw` with the default options and 120 as the degree of the collocation polynomials (fixed independently of M_X).

In Figure 2 the final time $T = 1000$ is fixed and M_X increases. We can observe that, apart from very low values of M_X, the error reaches a barrier.[16] We performed the same experiment with $T = 10000$ and could make the same observation, although the barrier was smaller by about one order of magnitude. The barrier depends on the error due to the time truncation in (2.5). Indeed, Figure 3, where M_X is constant and T varies, shows that the LEs converge linearly (confirming what is explained in [2]). In Figure 2 the truncation error appears to dominate on the error due to the collocation.

For the dominant nontrivial exponent[17] of the periodic solution, we observe in Figure 3 that, for $M_X = 8$, the error seems to reach a barrier, indicating that more ODEs are necessary to reproduce the properties of the original RE more accurately, as it is reasonable to expect. In other experiments, we observed that, as T increases, error barriers are reached also for increasing values of M_X.

We showed here the results of the main approach only. We performed the same experiments also with the alternative approach of Remark 4.1, using, for the linearization, both the exact solutions (which are known for the chosen values of γ) and the numerical solutions computed by using the trapezoidal method. With the exact solutions, we obtained almost exactly the same values: this means that the solution of the ODE is a good enough approximation of the solution of the RE, and that exchanging the linearization and the collocation does not influence the results. However, when using the numerical solutions obtained via the trapezoidal method, the errors on the LEs were higher: in the experiment shown in Figure 2, the errors in the periodic case were one order of magnitude larger, while in the

[16] Note in Figure 2 that for $\gamma = 3$ the error is initially below the final barrier; we do not have an explanation of this phenomenon, but in Figure 3 for $\gamma = 3$ and $M_X = 8$ we can observe rather erratic behavior of the error when varying T, despite the fact that it has a linearly decreasing bound. Moreover, we remark that the value of M_X required to reach the error barrier for a given T depends, in general, on the specific equation and the specific values of its parameters.

[17] The trivial exponent 0 is always an LE for a periodic solution due to the translation invariance.

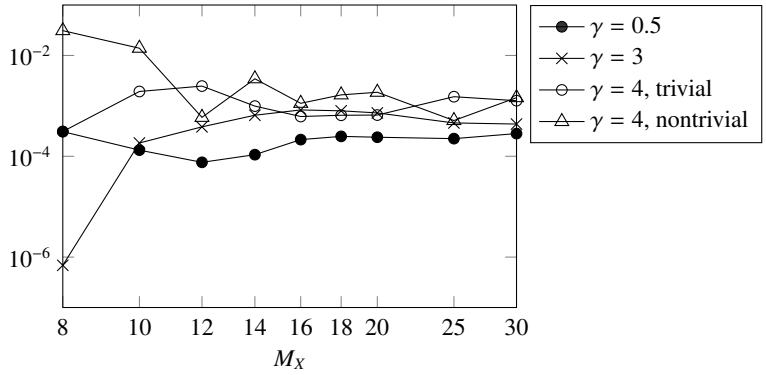

Figure 2. Absolute errors on the dominant LEs of the RE with quadratic nonlinearity (5.1) for values of γ corresponding to the stable trivial equilibrium ($\gamma = 0.5$), the stable nontrivial equilibrium ($\gamma = 3$) and the stable periodic orbit ($\gamma = 4$). For the last one, both the trivial and the dominant nontrivial exponents are shown. The errors are measured with respect to the exponents computed via `eigTMNpw`. The final time for `dqr` is $T = 1000$.

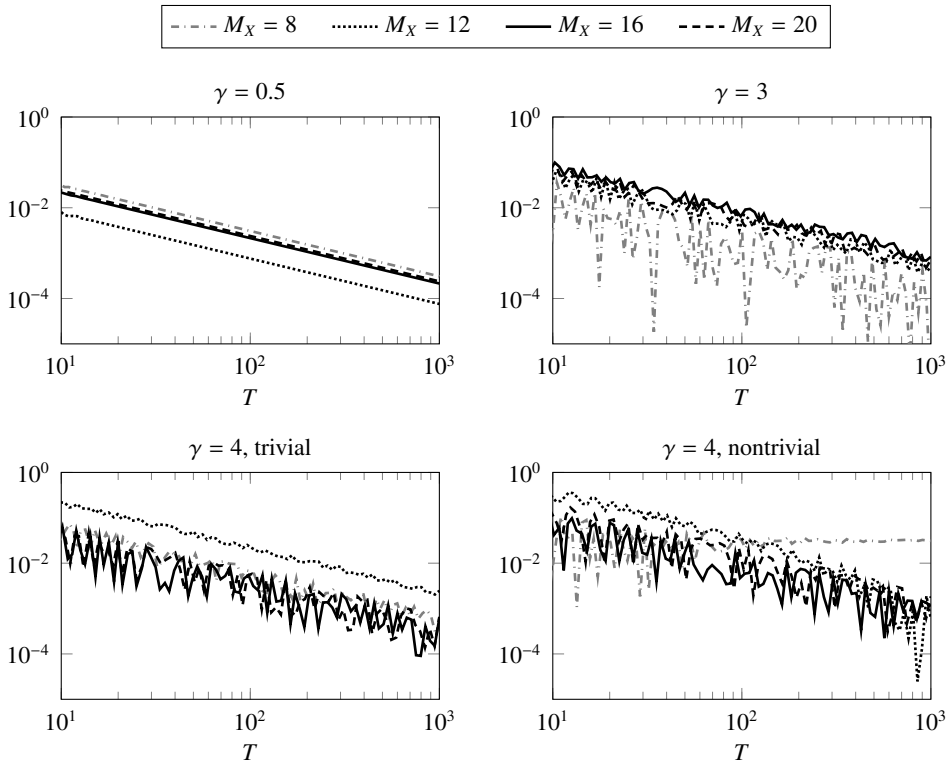

Figure 3. Absolute errors on the dominant LEs of the RE with quadratic nonlinearity (5.1) for values of γ corresponding to the stable trivial equilibrium ($\gamma = 0.5$), the stable nontrivial equilibrium ($\gamma = 3$) and the stable periodic orbit ($\gamma = 4$). For the last one, both the trivial and the dominant nontrivial exponents are shown. The errors are measured with respect to the exponents computed via `eigTMNpw`. The exponents are computed for $M_X \in \{8, 12, 16, 20\}$ as shown in the legend.

experiment of Figure 3 the errors reached barriers ranging between 10^{-2} and 10^{-1}. For these reasons, we henceforth use only the main approach as the more practical one.

Figure 4 (compare with [7, Figure 2.3]) presents, on the top row, the diagram of the first two dominant LEs of (5.1) when varying γ, computed with $M_X = 15$ and $T = 1000$, following previous experimental considerations. We can observe that the dominant LE is 0 at the expected Hopf bifurcation ($\gamma = 2 + \frac{\pi}{2}$), after which one LE is always 0 since periodic solutions appear. The dominant nontrivial exponent reaches 0 again for the expected period-doubling bifurcations at $\gamma \approx 4.32, 4.49, 4.53$, and it becomes positive for $\gamma \geq 4.55$, indicating the insurgence of a chaotic regime, which is compatible with what was obtained in [7]. Finally, for $\gamma \in [4.86, 4.9]$ other *stability islands* appear, corresponding to a branch of stable periodic solutions (appearing at $\gamma \approx 4.8665$) and the corresponding cascade of period-doubling bifurcations (at $\gamma \approx 4.8795, 4.8860$) leading back to chaos (starting at $\gamma \approx 4.8885$). As an example, Figure 4 (second and third row) shows some stable periodic solutions in the branches arising from the first and the second set of bifurcations. Observe that indeed the period approximately doubles at each bifurcation.

5.2. Egg cannibalism model

The second equation we consider is the egg cannibalism (toy) model from [38]:

$$x(t) = \frac{\gamma}{2} \int_{a_{\text{mat}}}^{a_{\max}} x(t-a)\mathrm{e}^{-x(t-a)}\,\mathrm{d}a, \tag{5.4}$$

with a_{mat} and $a_{\max}$ being, respectively, the constant maturation and maximum ages. Observe that (5.4) corresponds to (4.1) with $\tau_1 := a_{\text{mat}}$, $\tau_2 := a_{\max}$ and $f(x) := \frac{\gamma}{2} x\mathrm{e}^{-x}$. Also in this case, the equilibria and their stability properties are known, including the occurrence of a Hopf bifurcation for the nontrivial equilibrium at $\log(\gamma) = 1 + \frac{\pi}{2}$, although here the periodic solutions are not explicitly known; again, the presence of period-doubling bifurcations is experimentally known [4, 7, 8, 38].

Figure 5 (top row) presents the diagram of the first two dominant LEs of (5.4) when varying γ, with $a_{\text{mat}} = 1$ and $a_{\max} = 3$. The numerical parameters are $M_X = 15$, $T = 1000$, a tolerance of 10^{-6} for `dqr`, and `RelTol` $= 10^{-6}$ and `AbsTol` $= 10^{-7}$ for `ode45`. Similar to the previous example, the dominant exponent is 0 at the Hopf bifurcation, and one exponent remains 0 thereafter. The dominant nontrivial exponent reaches 0 again for the expected period-doubling bifurcations at $\log(\gamma) \approx 3.855$ ([8] finds $\log(\gamma) \approx 3.8777$ with $M_X = 20$ and $\log(\gamma) \approx 3.8763$ with $M_X = 40$, setting MatCont's tolerances to 10^{-10} for Newton's method and 10^{-6} for the calculation of the test functions for bifurcation points) and $\log(\gamma) \approx 4.54$, and it becomes positive for $\log(\gamma) \geq 4.66$, indicating chaos. Figure 5 (bottom row) shows some stable periodic solutions, confirming the (approximate) doubling of the period.

5.3. Simplified logistic Daphnia

The third and final equation is a simplified version of the Daphnia model with a logistic term as the growth of the resource, taken from [38]:

$$\begin{cases} b(t) = \beta S(t) \displaystyle\int_{a_{\text{mat}}}^{a_{\max}} b(t-a)\,\mathrm{d}a, \\ S'(t) = rS(t)\left(1 - \dfrac{S(t)}{K}\right) - \gamma S(t) \displaystyle\int_{a_{\text{mat}}}^{a_{\max}} b(t-a)\,\mathrm{d}a, \end{cases} \tag{5.5}$$

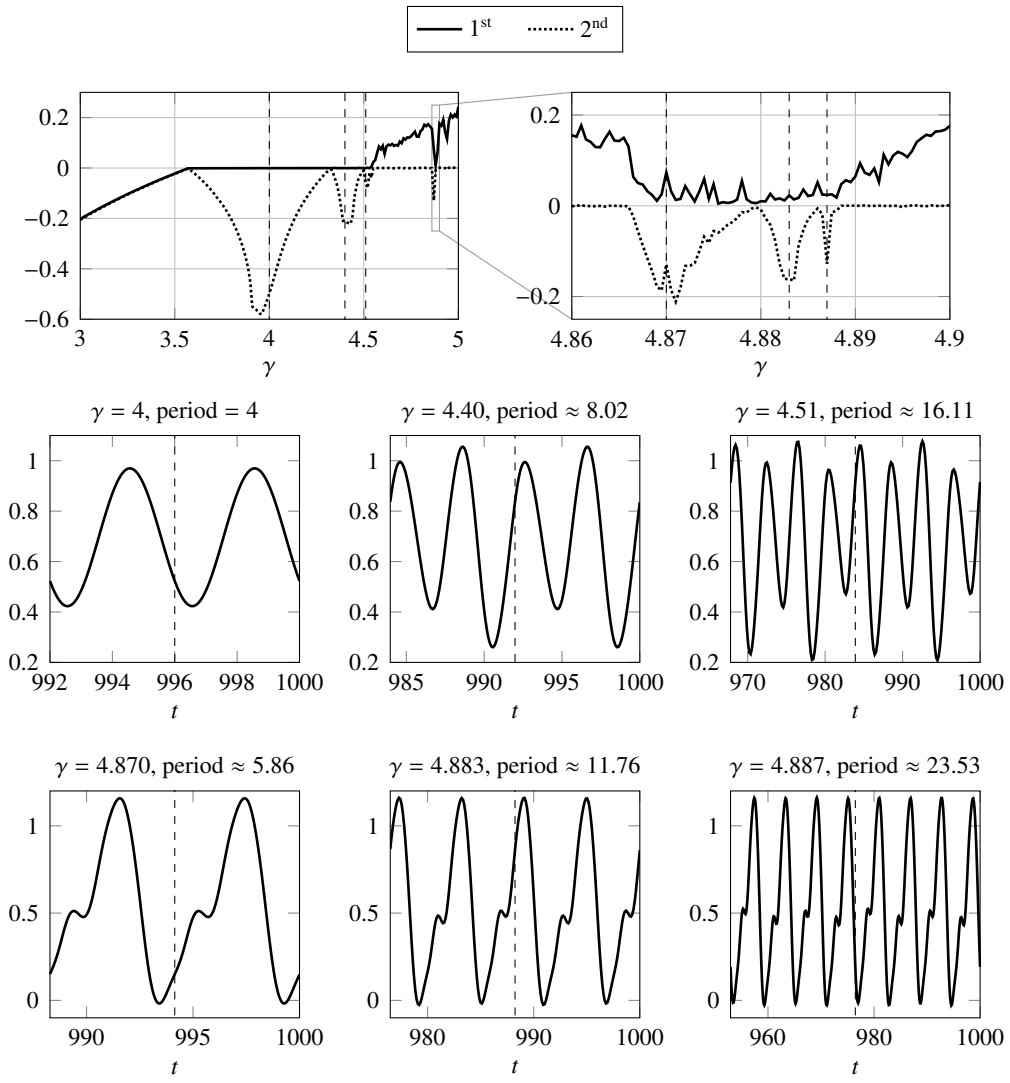

Figure 4. Diagram of the first two dominant (in descending order) LEs (top row) and solutions (other rows) of the RE with quadratic nonlinearity (5.1) when varying γ, computed with $M_X = 15$ and $T = 1000$. The solutions are computed via pseudospectral discretization with $M_X = 15$, starting from a constant initial value of 0.2. The final time of $T = 1000$ ensures sufficiently good convergence to the stable periodic solution. For each solution, the last two periods are shown, separated by a vertical dashed line. The values of γ and of the period are given above the diagrams; the values of γ are also marked by vertical dashed lines in the diagram of the LEs.

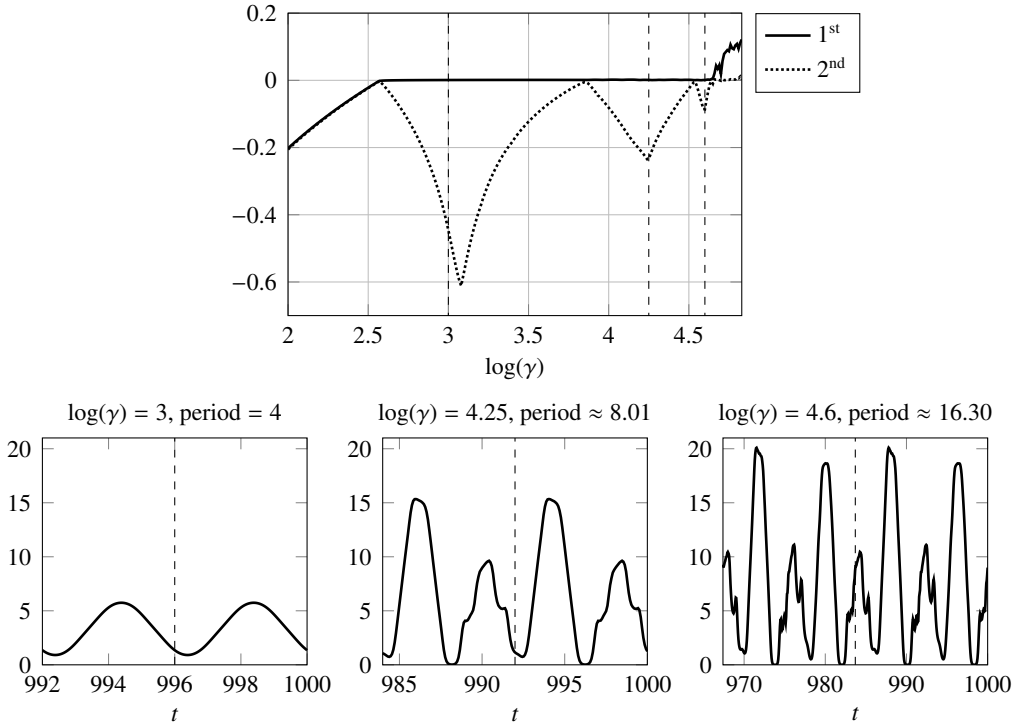

Figure 5. Diagram of the first two dominant (in descending order) LEs (top row) and solutions (bottom row) of the egg cannibalism RE (5.4) with $a_{\text{mat}} = 1$ and $a_{\max} = 3$, when varying γ, computed with $M_X = 15$ and $T = 1000$. The solutions are computed via pseudospectral discretization with $M_X = 15$, starting from a constant initial value of 0.2. The final time of $T = 1000$ ensures sufficiently good convergence to the stable periodic solution. For each solution, the last two periods are shown, separated by a vertical dashed line. The values of γ and of the period are given above the diagrams; the values of γ are also marked by vertical dashed lines in the diagram of LEs.

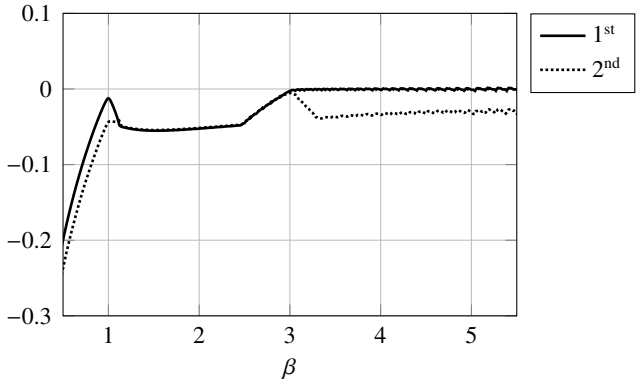

Figure 6. Diagram of the first two dominant (in descending order) LEs of the simplified logistic Daphnia equation (5.5) with $a_{\text{mat}} = 3$, $a_{\max} = 4$ and $r = K = \gamma = 1$, when varying β, computed with $M_X = 15$ and $T = 1000$.

where b is the birth rate of the consumer population, S is the density of the resource, r and K are, respectively, the growth rate and the carrying capacity of the resource, and a_{mat} and $a_{\max}$ have the same meaning as in Section 5.2.[18] Equation (5.5) corresponds to (4.2) with $\tau_1 := a_{\text{mat}}$, $\tau_2 := a_{\max}$, $f_1(x) := \beta x$, $f_2(x) := -\gamma x$ and $g(y) := ry(1 - \frac{y}{K})$. The equilibria are known, along with the stability properties of the trivial (zero and consumer-free) ones; in particular, the consumer-free equlibrium exchanges stability with the nontrivial equilibrium in a transcritical bifurcation at $\beta = (K(a_{\max} - a_{\text{mat}}))^{-1}$; moreover, when varying β, the nontrivial equilibrium is experimentally known to undergo a Hopf bifurcation [4, 38, 39].

The diagram of the first two dominant LEs of (5.5) when varying β is shown in Figure 6. The values of the other model parameters are $a_{\text{mat}} = 3$, $a_{\max} = 4$ and $r = K = \gamma = 1$. The numerical parameters are $M_X = M_Y = 15$, $T = 1000$, a tolerance of 10^{-6} for `dqr`, and `RelTol` $= 10^{-4}$ and `AbsTol` $= 10^{-5}$ for `ode45`. We can observe a spike at $\beta = 1$ (albeit not touching the value 0), corresponding to the known transcritical bifurcation, while the Hopf bifurcation seems to happen for $\gamma \approx 3$ ([4] finds $\gamma \approx 3.0161$ with $M_X = 10$ and MatCont's tolerances set to 10^{-10}). We continued the experiment for values of β higher than those shown in Figure 6, but we did not find other bifurcations.

Compared with the previous examples, the diagram seems less accurate (observe the spike corresponding to the transcritical bifurcation and the trivial LE after the Hopf bifurcation). The explanation for this phenomenon is still unknown. In this example, we have increased the tolerances for `ode45` in order to improve the computation times; however, for $\beta = 1$ the dominant LE differs absolutely from the one computed with `RelTol` $= 10^{-6}$ and `AbsTol` $= 10^{-7}$ (as in the previous examples) by less than 10^{-7} and is thus still substantially far from 0 (as a further example, for $\beta = 5$ the absolute difference is larger but still less than 10^{-5}). Moreover, as β increases, the periodic solution presents flat regions followed by spikes, which may suggest that the equation is becoming stiff; however, we tried replacing `ode45` with MATLAB's `ode23s`, implementing a modified Rosenbrock formula of order 2 for stiff ODEs [27], with no substantial changes.

[18]Note that the second term on the right-hand side of the equation for S in (5.5) can be rewritten as $\gamma b(t)/\beta$, rendering that equation an ODE. This does not bring any simplification since the integral term is computed for the first equation anyway. We prefer to keep the form of (5.5) because it comes from a more general class where the fertility and consumption rates are not constant, but, rather, are functions of the age and the size of the individuals (see (1) in [38]).

6. Concluding remarks

In this work, we have provided the first method, to our knowledge, for computing LEs of REs and coupled equations. The proposed method appears to be effective when applied to examples with known properties; however, since the nature of our study has been purely computational, further investigation into the method's convergence properties is required. As far as efficiency is concerned, LEs are notoriously expensive to compute [2], and that is true also in this case; the computational cost depends linearly on T, while its relation with M_X and M_Y is currently unclear from the experiments, even though it is expected to be of order 4, according to (2.3).

The next step in our research is to tackle the problem following the approach of [2]; as recalled in Section 1, this involves the reformulation of the equation (RE or coupled equation, in our case) in a Hilbert space and the rigorous definition of LEs and the DQR in the new setting. The technique of [3] and of the present work, however, is a rather general approach which can also be applied to other kinds of equations (e.g., certain classes of partial differential equations of interest for mathematical biology [40]), as anticipated in [3] and according to the *pragmatic* point of view discussed in [7].

Use of AI tools declaration

The authors declare they have not used Artificial Intelligence (AI) tools in the creation of this article.

Acknowledgments

The authors are members of INdAM research group GNCS and of UMI research group "Modellistica socio-epidemiologica". This work was partially supported by the Italian Ministry of University and Research (MUR) through the PRIN 2020 project (No. 2020JLWP23) "Integrated Mathematical Approaches to Socio-Epidemiological Dynamics" (CUP: E15F21005420006), and by the GNCS 2023 project "Sistemi dinamici e modelli di evoluzione: tecniche funzionali, analisi qualitativa e metodi numerici" (CUP: E53C22001930001).

Conflict of interest

The authors declare there is no conflict of interest.

References

1. O. Diekmann, S. M. Verduyn Lunel, Twin semigroups and delay equations, *J. Differ. Equ.*, **286** (2021), 332–410. https://doi.org/10.1016/j.jde.2021.02.052
2. D. Breda, E. Van Vleck, Approximating Lyapunov exponents and Sacker–Sell spectrum for retarded functional differential equations, *Numer. Math.*, **126** (2014), 225–257. https://doi.org/10.1007/s00211-013-0565-1
3. D. Breda, S. Della Schiava, Pseudospectral reduction to compute Lyapunov exponents of delay differential equations, *Discrete Contin. Dyn. Syst. Ser. B*, **23** (2018), 2727–2741. https://doi.org/10.3934/dcdsb.2018092

4. D. Breda, O. Diekmann, M. Gyllenberg, F. Scarabel, R. Vermiglio, Pseudospectral discretization of nonlinear delay equations: New prospects for numerical bifurcation analysis, *SIAM J. Appl. Dyn. Syst.*, **15** (2016), 1–23. https://doi.org/10.1137/15M1040931
5. L. Dieci, E. S. Van Vleck, LESLIS and LESLIL: Codes for approximating Lyapunov exponents of linear systems, 2004, URL `https://dieci.math.gatech.edu/software-les.html`.
6. L. Dieci, M. S. Jolly, E. S. Van Vleck, Numerical techniques for approximating Lyapunov exponents and their implementation, *J. Comput. Nonlinear Dynam.*, **6** (2011), 011003. https://doi.org/10.1115/1.4002088
7. D. Breda, O. Diekmann, D. Liessi, F. Scarabel, Numerical bifurcation analysis of a class of nonlinear renewal equations, *Electron. J. Qual. Theory Differ. Equ.*, **2016** (2016), 65. https://doi.org/10.14232/ejqtde.2016.1.65
8. F. Scarabel, O. Diekmann, R. Vermiglio, Numerical bifurcation analysis of renewal equations via pseudospectral approximation, *J. Comput. Appl. Math.*, **397** (2021), 113611. https://doi.org/10.1016/j.cam.2021.113611
9. L. Y. Adrianova, *Introduction to Linear Systems of Differential Equations*, no. 146 in Transl. Math. Monogr., American Mathematical Society, Providence, RI, 1995.
10. G. A. Leonov, N. V. Kuznetsov, Time-varying linearization and the Perron effects, *Internat. J. Bifur. Chaos Appl. Sci. Engrg.*, **17** (2007), 1079–1107. https://doi.org/10.1142/S0218127407017732
11. L. Barreira, C. Valls, Stability of the Lyapunov exponents under perturbations, *Ann. Funct. Anal.*, **8** (2017), 398–410. https://doi.org/10.1215/20088752-2017-0005
12. L. Dieci, E. S. Van Vleck, Lyapunov spectral intervals: Theory and computation, *SIAM J. Numer. Anal.*, **40** (2002), 516–542. https://doi.org/10.1137/S0036142901392304
13. G. Benettin, L. Galgani, A. Giorgilli, J. M. Strelcyn, Lyapunov characteristic exponents for smooth dynamical systems and for Hamiltonian systems; a method for computing all of them. Part 1: Theory, *Meccanica*, **15** (1980), 9–20. https://doi.org/10.1007/BF02128236
14. G. Benettin, L. Galgani, A. Giorgilli, J.-M. Strelcyn, Lyapunov characteristic exponents for smooth dynamical systems and for Hamiltonian systems; a method for computing all of them. Part 2: Numerical application, *Meccanica*, **15** (1980), 21–30. https://doi.org/10.1007/BF02128237
15. D. Breda, Nonautonomous delay differential equations in Hilbert spaces and Lyapunov exponents, *Differential Integral Equations*, **23** (2010), 935–956. https://doi.org/10.57262/die/1356019118
16. J. D. Farmer, Chaotic attractors of an infinite-dimensional dynamical system, *Phys. D.*, **4** (1982), 366–393. https://doi.org/10.1016/0167-2789(82)90042-2
17. M. D. Chekroun, M. Ghil, H. Liu, S. Wang, Low-dimensional Galerkin approximations of nonlinear delay differential equations, *Discrete Contin. Dyn. Syst.*, **36** (2016), 4133–4177. https://doi.org/10.3934/dcds.2016.36.4133
18. O. Diekmann, P. Getto, M. Gyllenberg, Stability and bifurcation analysis of Volterra functional equations in the light of suns and stars, *SIAM J. Math. Anal.*, **39** (2008), 1023–1069. https://doi.org/10.1137/060659211

19. O. Diekmann, S. A. van Gils, S. M. Verduyn Lunel, H.-O. Walther, *Delay Equations: Functional-, Complex- and Nonlinear Analysis*, no. 110 in Appl. Math. Sci., Springer, New York, 1995. https://doi.org/10.1007/978-1-4612-4206-2
20. J. K. Hale, S. M. Verduyn Lunel, *Introduction to Functional Differential Equations*, no. 99 in Appl. Math. Sci., Springer, New York, 1993. https://doi.org/10.1007/978-1-4612-4342-7
21. J. Ripoll, J. Font, Numerical approach to an age-structured Lotka–Volterra model, *Math. Biosci. Eng.*, **20** (2023), 15603–15622. https://doi.org/10.3934/mbe.2023696
22. L. N. Trefethen, *Spectral Methods in MATLAB*, Software Environ. Tools, Society for Industrial and Applied Mathematics, Philadelphia, 2000. https://doi.org/10.1137/1.9780898719598
23. J.-P. Berrut, L. N. Trefethen, Barycentric Lagrange interpolation, *SIAM Rev.*, **46** (2004), 501–517. https://doi.org/10.1137/S0036144502417715
24. C. W. Clenshaw, A. R. Curtis, A method for numerical integration on an automatic computer, *SIAM J. Numer. Anal.*, **2** (1960), 197–205. https://doi.org/10.1007/BF01386223
25. L. N. Trefethen, Is Gauss quadrature better than Clenshaw–Curtis?, *SIAM Rev.*, **50** (2008), 67–87. https://doi.org/10.1137/060659831
26. J. R. Dormand, P. J. Prince, A family of embedded Runge–Kutta formulae, *J. Comput. Appl. Math.*, **6** (1980), 19–26. https://doi.org/10.1016/0771-050X(80)90013-3
27. L. F. Shampine, M. W. Reichelt, The MATLAB ODE suite, *SIAM J. Sci. Comput.*, **18** (1980), 1–22. https://doi.org/10.1137/S1064827594276424
28. E. Messina, E. Russo, A. Vecchio, A stable numerical method for Volterra integral equations with discontinuous kernel, *J. Math. Anal. Appl.*, **337** (2008), 1383–1393. https://doi.org/10.1016/j.jmaa.2007.04.059
29. D. Breda, D. Liessi, Approximation of eigenvalues of evolution operators for linear renewal equations, *SIAM J. Numer. Anal.*, **56** (2018), 1456–1481. https://doi.org/10.1137/17M1140534
30. D. Breda, D. Liessi, R. Vermiglio, Piecewise discretization of monodromy operators of delay equations on adapted meshes, *J. Comput. Dyn.*, **9** (2022), 103–121. https://doi.org/10.3934/jcd.2022004
31. D. Breda, D. Liessi, R. Vermiglio, A practical guide to piecewise pseudospectral collocation for Floquet multipliers of delay equations in MATLAB, submitted.
32. A. Bellen, Z. Jackiewicz, R. Vermiglio, M. Zennaro, Natural continuous extensions of Runge–Kutta methods for Volterra integral equations of the second kind and their application, *Math. Comp.*, **52** (1989), 49–63. https://doi.org/10.1090/S0025-5718-1989-0971402-3
33. R. Vermiglio, On the stability of Runge–Kutta methods for delay integral equations, *Numer. Math.*, **61** (1992), 561–577. https://doi.org/10.1007/BF01385526
34. H. Brunner, Collocation and continuous implicit Runge–Kutta methods for a class of delay Volterra integral equations, *J. Comput. Appl. Math.*, **53** (1994), 61–72. https://doi.org/10.1016/0377-0427(92)00125-S
35. A. Andò, Convergence of collocation methods for solving periodic boundary value problems for renewal equations defined through finite-dimensional boundary conditions, *Comput. Math. Methods*, **3** (2021), e1190. https://doi.org/10.1002/cmm4.1190

36. A. Andò, D. Breda, Piecewise orthogonal collocation for computing periodic solutions of coupled delay equations, *Appl. Numer. Math.*. https://doi.org/10.1016/j.apnum.2023.05.010

37. A. Andò, D. Breda, Piecewise orthogonal collocation for computing periodic solutions of renewal equations, submitted.

38. D. Breda, O. Diekmann, S. Maset, R. Vermiglio, A numerical approach for investigating the stability of equilibria for structured population models, *J. Biol. Dyn.*, **7** (2013), 4–20. https://doi.org/10.1080/17513758.2013.789562

39. D. Breda, D. Liessi, Approximation of eigenvalues of evolution operators for linear coupled renewal and retarded functional differential equations, *Ric. Mat.*, **69** (2020), 457–481. https://doi.org/10.1007/s11587-020-00513-9

40. L. M. Abia, Ó. Angulo, J. C. López-Marcos, M. A. López-Marcos, Numerical integration of an age-structured population model with infinite life span, *Appl. Math. Comput.*, **434** (2022), 127401. https://doi.org/10.1016/j.amc.2022.127401

AIMS Press